

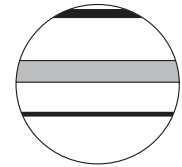
Original

McCarroll, D.; Loader, N.J.; Jalkanen, R.; Gagen, M.H.; Grudd, H.; Gunnarson, B.E.; Kirchhefer, A.J.; Friedrich, M.; Linderholm, H.W.; Lindholm, M.; Boettger, T.; Los, S.O.; Remmele, S.; Kononov, Y.M.; Yamazaki, Y.H.; Young, G.H.F.; Zorita, E.:


A 1200-year multiproxy record of tree growth and summer temperature at the northern pine forest limit of Europe

In: The Holocene (2013) SAGE Publications

DOI: 10.1177/0959683612467483



A 1200-year multiproxy record of tree growth and summer temperature at the northern pine forest limit of Europe

The Holocene
23(4) 471–484
© The Author(s) 2013
Reprints and permission:
sagepub.co.uk/journalsPermissions.nav
DOI: 10.1177/0959683612467483
hol.sagepub.com


Danny McCarroll,¹ Neil J Loader,¹ Risto Jalkanen,² Mary H Gagen,¹ Håkan Grudd,³ Björn E Gunnarson,³ Andreas J Kirchhefer,⁴ Michael Friedrich,⁵ Hans W Linderholm,⁶ Markus Lindholm,² Tatjana Boettger,⁷ Sietse O Los,¹ Sabine Remmele,⁵ Yuri M Kononov,⁸ Yasuhiro H Yamazaki,^{9,10} Giles HF Young¹ and Eduardo Zorita¹¹

Abstract

Combining nine tree growth proxies from four sites, from the west coast of Norway to the Kola Peninsula of NW Russia, provides a well replicated (> 100 annual measurements per year) mean index of tree growth over the last 1200 years that represents the growth of much of the northern pine timberline forests of northern Fennoscandia. The simple mean of the nine series, z-scored over their common period, correlates strongly with mean June to August temperature averaged over this region ($r = 0.81$), allowing reconstructions of summer temperature based on regression and variance scaling. The reconstructions correlate significantly with gridded summer temperatures across the whole of Fennoscandia, extending north across Svalbard and south into Denmark. Uncertainty in the reconstructions is estimated by combining the uncertainty in mean tree growth with the uncertainty in the regression models. Over the last seven centuries the uncertainty is < 4.5% higher than in the 20th century, and reaches a maximum of 12% above recent levels during the 10th century. The results suggest that the 20th century was the warmest of the last 1200 years, but that it was not significantly different from the 11th century. The coldest century was the 17th. The impact of volcanic eruptions is clear, and a delayed recovery from pairs or multiple eruptions suggests the presence of some positive feedback mechanism. There is no clear and consistent link between northern Fennoscandian summer temperatures and solar forcing.

Keywords

climate change, 'Little Ice Age', solar forcing, tree rings, volcanic forcing

Received 12 July 2012; revised manuscript accepted 8 October 2012

Introduction

As the evidence for anthropogenically induced global warming has accumulated, it has become increasingly important to reconstruct the climate of the past at high temporal resolution. Viewing recent and projected warming within the context of natural variability is vital because this is the only way to determine whether the magnitude and rate of recent changes are unprecedented under present environmental boundary conditions (Intergovernmental Panel on Climate Change (IPCC), 2007; Jones et al., 2009; Mann et al., 1999). High temporal resolution climate reconstructions can also be compared with estimates of the natural drivers of the climate system, including records of variations in solar activity and of volcanic sulphate concentrations. This would allow estimates to be made of the sensitivity of the climate system to natural forcings. Where it can be demonstrated that palaeoclimate reconstructions are representative of a sufficiently large area, they can also potentially be used to test the veracity of the complex General Circulation Models (GCM) used to predict the future evolution of Earth's climate, and in particular to constrain the very large uncertainty in the estimates of the sensitivity of the climate system to rising levels of greenhouse gases (Edwards et al., 2007; Knutti and Hegerl, 2008; McCarroll, 2010).

There are many potential natural archives of palaeoclimate information, but trees are one of the best (Hughes, 2002). Where ring boundaries are clear, tree rings can be measured and cross-matched to produce accurately dated and annually resolved

chronologies. Although there are few suitable tree species that live for more than a few hundred years, chronologies can be extended using building timbers, standing dead wood or 'subfossil' trees recovered from lakes, bogs and river sediments. In areas where climate exerts a strong control on tree growth, the tree ring width chronologies, together with other physical and chemical proxies, can provide one of the most powerful methods for reconstructing the climate of the past. Measurements can be replicated, and the link to climate quantified by direct comparison with

¹Swansea University, UK

²Finnish Forest Research Institute, Rovaniemi Research Unit, Finland

³Stockholm University, Sweden

⁴University of Tromsø, Norway

⁵University of Hohenheim, Germany

⁶University of Gothenburg, Sweden

⁷Helmholtz Centre for Environment, Germany

⁸Russian Academy of Science, Russia

⁹Newcastle University, UK

¹⁰University of Oxford, UK

¹¹GKSS Research Centre, Germany

Corresponding author:

Danny McCarroll, Department of Geography, Swansea University, Singleton Park, Swansea SA2 8PP, UK.
Email: d.mccarroll@swansea.ac.uk

instrumental measurements, so the palaeoclimate reconstructions can be furnished with realistic uncertainty estimates.

Northern Fennoscandia has long been recognized as a region where it is possible to produce long and climatically sensitive tree ring chronologies (Briffa et al., 1990; Eronen et al., 2002; Grudd, 2008; Grudd et al., 2002; Gunnarson and Linderholm 2002; Gunnarson et al., 2011; Helama et al., 2002; Kirchhefer, 2001; Kononov et al., 2009; Lindholm et al., 2009). In central and southern Sweden and Finland there are sites where trees are sensitive to variations in precipitation, but towards the northern timberline Scots pine (*Pinus sylvestris* L.) growth is strongly controlled by summer temperature. Dendroclimatological research in this region has recently been reviewed by Linderholm et al. (2010) and many of the published series have been combined and analysed by Gouirand et al. (2008). The latter concluded that summer temperatures in Fennoscandia could be represented by a relatively small number of temperature-sensitive chronologies, while Linderholm et al. (2010: 107) suggest that 'it is not beyond reach to extend the tree-ring data from the key sites (or similar) up to the present and back to ca AD 1000'. It is the update, extension and regional reconstruction of palaeoclimate for northern Fennoscandia that form the central aims of this paper.

Sites and methods

Four sites were selected, forming a 750 km transect across northern Fennoscandia from the west coast of Norway to the Kola

Peninsula in Russia (Figure 1). In each case there was proven potential for producing a chronology that would approach 1000 years in length with a known sensitivity to summer temperature. Forfjorddalen is located in maritime Northern Norway (68.79°N, 15.73°E, 40–160 m a.s.l.) about 170 km west of the more alpine site at Torneträsk in Sweden (68.21–68.31°N, 19.45–19.80°E, 350–450 m a.s.l.). Laanila in Inari, Finland (68.47–68.52°N, 27.27–27.40°E, 220–310 m a.s.l.), is located 320 km east from Torneträsk, and the Khibiny site in Kola peninsula, NW Russia (67.63–67.83°N, 33.22–34.25°E, 250–400 m a.s.l.) 230 km SE from Laanila.

Ring widths were measured and carefully cross-dated at all sites and at three sites late wood maximum density was also measured, using standard methods (Bergsten et al., 2001; Schweingruber, 1988). Ring width and density series were detrended using Regional Curve Standardisation (Esper et al., 2003) to preserve low frequency variability and chronologies produced by calculating the robust (biweight) mean of the indices. The Torneträsk data of Grudd (2008) have been updated and reprocessed using a signal-free approach by Melvin et al. (2012). At Khibiny density was replaced with a modified version of the novel and less expensive alternative based on blue reflectance/intensity (Campbell et al., 2007, 2011; McCarroll et al., 2002) and detrending was achieved using 67% splines. At Laanila a 1200-year record of annual height growth (detrended using 67% splines relative to series length) is also included (Lindholm et al., 2009, 2011). Height growth occurs early in the growing season, responding to the temperature of the

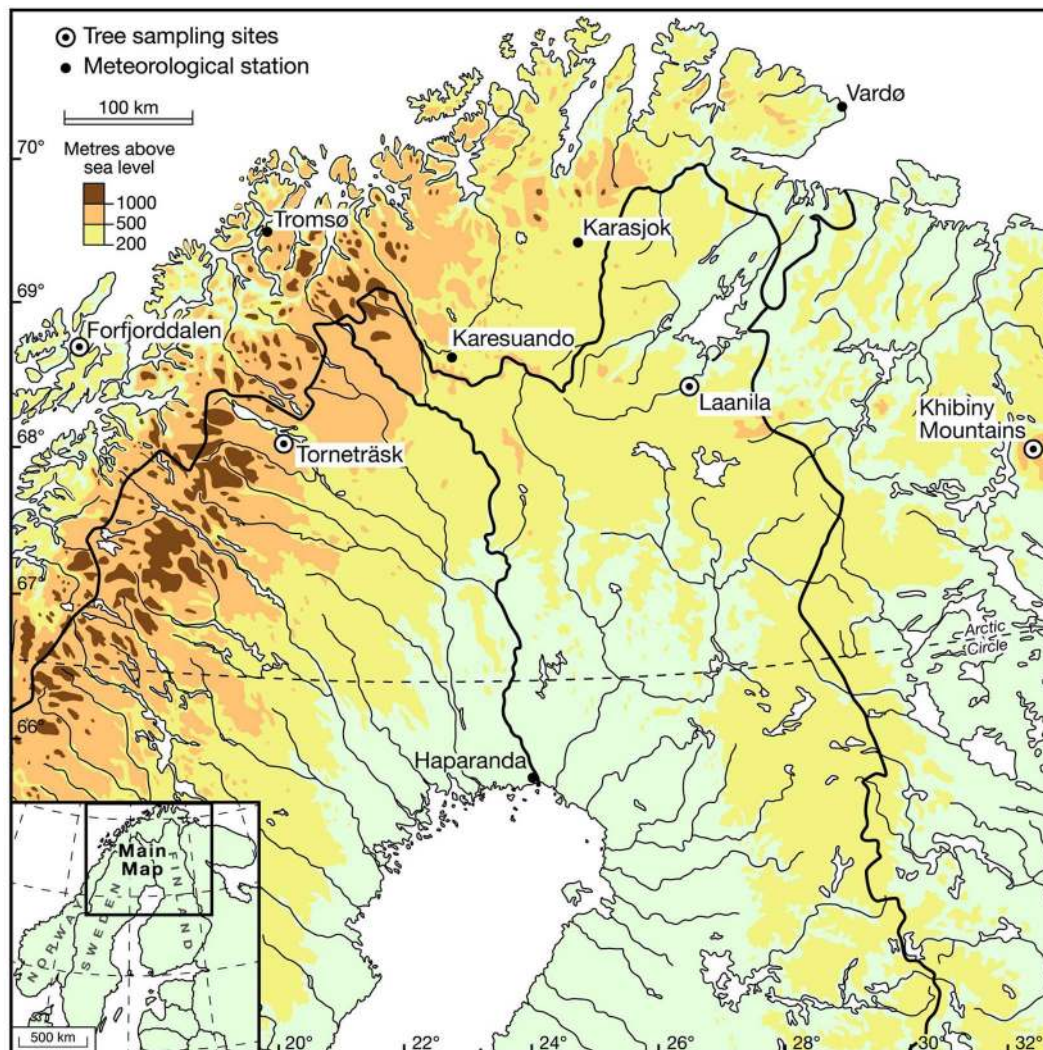


Figure 1. Map of the study area.

previous summer, when the bud is formed (Salminen and Jalankainen, 2005). The height proxy data are therefore shifted by 1 yr to align this environmental signal with that of the ring width and density proxies. The data are archived at the NOAA paleoclimate data center and full details of the sites and sampling strategies are included elsewhere (Forfjorddalen: Kirchhefer, 2001; Young et al., 2010, 2012; Torneträsk: Grudd, 2008, Loader et al., 2012; Melvin et al., 2012; Laanila: Gagen et al., 2007; Lindholm et al., 2009, 2011; Khibiny: Kononov et al., 2009).

The individual site chronologies were first normalised (*z*-scored) and combined to provide a regional overview of variations in tree growth, and then the overall mean chronology was calibrated using a network of climate stations to provide reconstructions of June to August (JJA) mean temperature using a combined regression and scaling approach. Replication varies over time and between proxies and is higher for ring widths than for densities (Figure 2). The total number of samples included in the combined data set for each year exceeds 400 for all but the last few years of the calibration period, exceeds 144 over the last millennium and throughout the record does not fall below 100 (Figure 2a). Since ring width and density or blue reflectance can be measured on the same wood cores, the total number of cores is somewhat less, but still very large, exceeding 300 for all but the last decade of the calibration period (minimum 79 in AD 2005), 90 throughout the last millennium and 79 throughout the whole record (Figure 2b).

Results

Tree growth

The shortest record is the ring width series from Forfjorddalen, beginning in AD 1082 and several records finish in AD 2005, so for ease of comparison all of the proxies were *z*-scored over this common period (Figure 3). When all nine series are compared across their full length, at annual resolution, the strongest

intercorrelations (Pearson's *r*) are found between different proxies measured at the same site or similar proxies measured at adjacent sites (Table 1). The weakest correlations are found between different proxies measured at distant sites. All of the correlation coefficients are positive, and because of the large sample size even relatively low *r*-values are statistically significant. The only pair that is not significantly correlated (at $p < 0.05$) represents different parameters measured at the two most distant sites (Forfjorddalen ring width and Khibiny blue reflectance). The average correlation between all possible proxy pairs over their full periods is 0.34 and over the common period it is 0.35. Ring width and density from Forfjorddalen have the lowest average correlation with all other proxies and with the mean. Laanila density has the highest average correlation. It is notable that the two novel proxy chronologies; Laanila height and Khibiny blue reflectance, correlate well with the other proxies, height correlating more strongly with ring width and blue reflectance with density.

The seven series treated using Regional Curve Standardization (RCS) (height increment and blue reflectance excluded) can be compared to determine whether the lowest-frequency components are similar between proxies and between sites. This also tests whether including the two non-RCS treated series will result in a loss of very low-frequency climatic information. Over the common period, four of the RCS chronologies have no long-term trend and three (Forfjorddalen ring width, Torneträsk density and Khibiny ring width) have very slight rising trends (0.08, 0.05 and 0.02 SD units per century, $p < 0.05$), which although statistically significant account for less than 1% of the variance in each series. The mean of the seven RCS chronologies (re-scaled) shows a slight but significant rise over the common period (0.03 SD units per century, $r = 0.09$, $p < 0.05$). Including the two non-RCS chronologies produces a mean curve (re-scaled) which correlates very strongly with the mean of the RCS chronologies ($r = 0.97$) and the rising trend is preserved (0.03 SD units per century, $r = 0.08$,

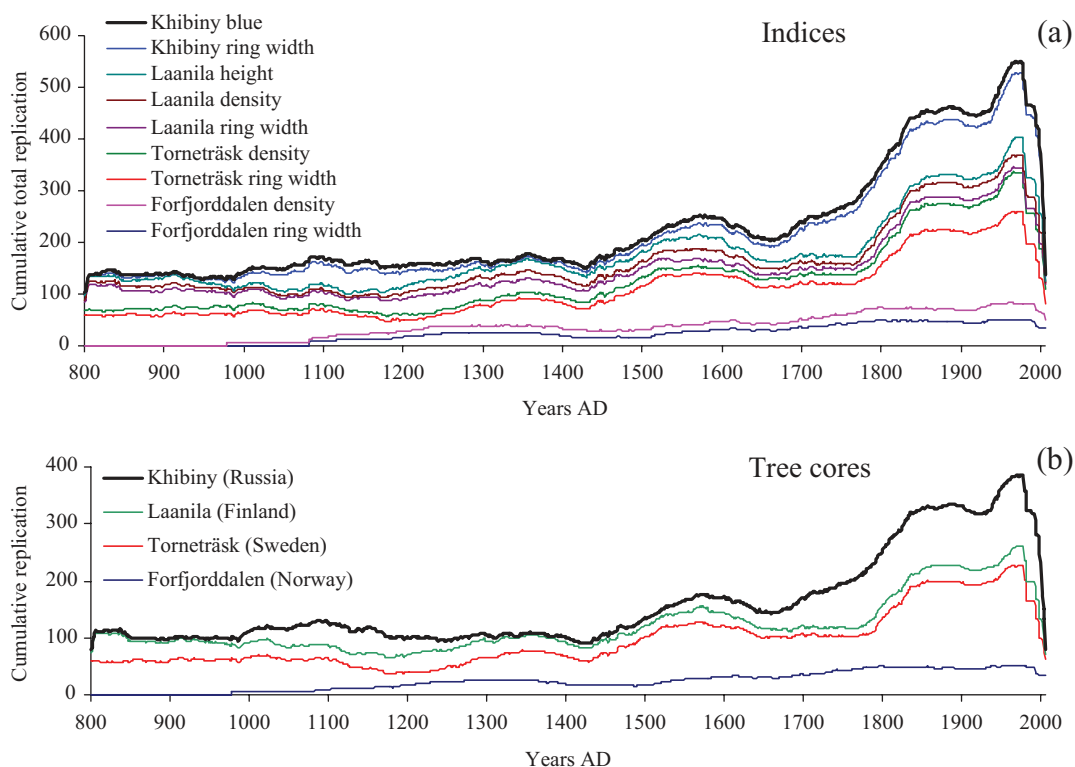


Figure 2. Sample replication plotted as cumulative totals for data (a) and tree cores (b). The lines fall in the order indicated in the legend, with Forfjorddalen at the bottom. The top line thus represents the total number of indices (a) or tree cores (b) included in the combined data set for each year.

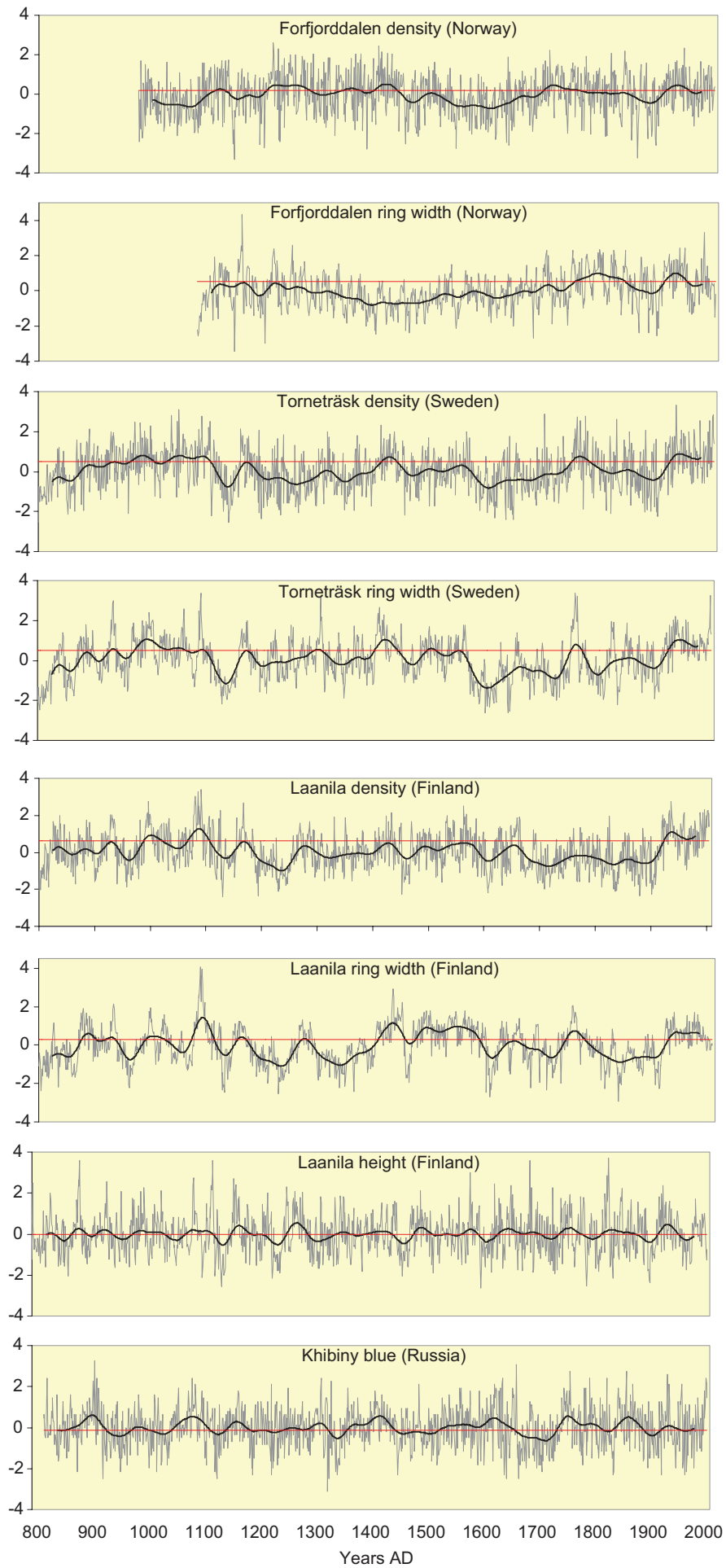


Figure 3. (Continued)

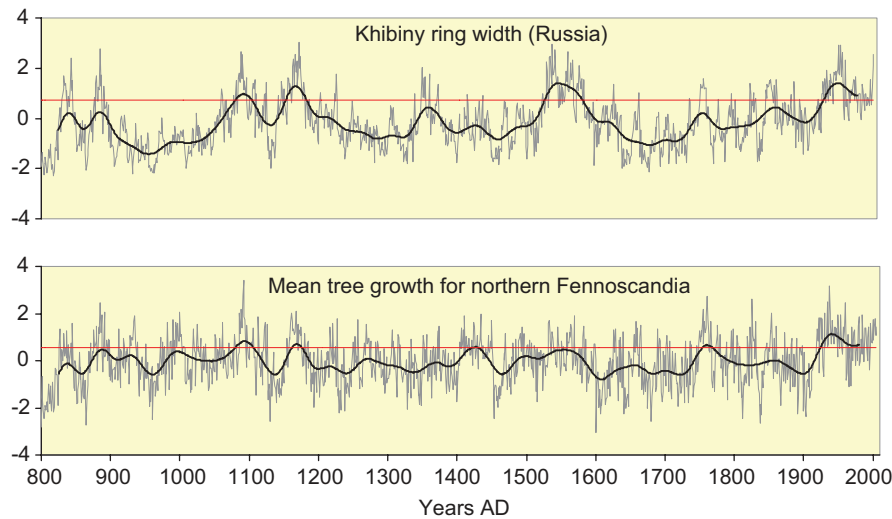


Figure 3. The nine chronologies z-scored over the common period (AD 1082 to AD 2005) and displayed at annual resolution and after smoothing with a 50 yr Gaussian filter. Units are standard deviations. The horizontal red line is the 20th century mean (colour figure available online).

Table 1. Correlation (Pearson’s *r*) between the proxy series and with the mean of all of the proxies (Mean) over the full period (upper panel) and over the common period (lower panel).

	F-D	F-RW	T-D	T-RW	L-D	Full period AD 800 to AD 2005				Mean
						L-RW	L-H	K-B	K-RW	
F-D		0.51	0.49	0.24	0.31	0.07	0.22	0.34	0.04	0.55
F-RW	0.51		0.28	0.24	0.16	0.09	0.27	0.14	0.15	0.48
T-D	0.53	0.28		0.57	0.57	0.36	0.25	0.46	0.22	0.72
T-RW	0.26	0.24	0.56		0.49	0.56	0.35	0.25	0.40	0.72
L-D	0.33	0.16	0.59	0.50		0.62	0.40	0.54	0.41	0.79
L-RW	0.06	0.09	0.39	0.56	0.65		0.45	0.28	0.49	0.70
L-H	0.21	0.27	0.25	0.35	0.41	0.45		0.31	0.30	0.61
K-B	0.35	0.14	0.50	0.30	0.57	0.30	0.35		0.32	0.63
K-RW	<u>0.01</u>	0.15	0.29	0.47	0.47	0.52	0.31	0.35		0.59
Mean	<u>0.56</u>	0.48	0.75	0.72	0.80	0.68	0.61	0.66	0.61	

Common period AD 1082 to AD 2005

Notes:

Values that are not statistically significant ($p > 0.05$, against a Gaussian white noise null-hypothesis) are underlined.
 F: Forfjorddalen; T: Torneträsk; L: Laanila; K: Khibiny; D: density; RW: ring width; H: height increment; B: blue reflectance.

$p < 0.05$). There seems to be little justification for excluding the Laanila height and Khibiny blue reflectance results in further analyses. Including these two series also has the advantage of retaining the spatial symmetry of the sampling and also increases the sample size and therefore reduces the uncertainty in the estimates of both mean tree growth and of past climate. Given the positive correlations between the nine proxy records it is reasonable to combine them to produce a simple average of the z-scores, providing a 1200-year mean index of tree growth that represents the latitudinal pine forest limit of the whole of northern Fennoscandia (Figure 4). Since the annual mean values are based on a sample of six to nine chronologies, uncertainty in the mean annual values can be expressed simply using 95% confidence limits (between 2.57 and 2.31 standard errors of the mean).

The 20th century has the highest mean growth index even though the mean value for the first decade is the second lowest for any calendar decade of the past millennium. The 20th century mean is significantly different (2-tailed student’s *t*-tests, $p < 0.05$) from every century except for the 11th ($p = 0.06$), when tree growth was also high. Growth indices were at their lowest during the 17th century. The calendar decade with highest mean growth index is the AD 1930s, followed by the AD 1160s. The calendar

decades with lowest growth indices in the entire record are the first 20 years of the 9th century, and the lowest of the last millennium was the first decade of the 17th century. The highest annual mean growth index of the entire record falls in AD 1092 and the second highest in AD 1937. The lowest value falls in AD 1601.

Calibration and palaeoclimate reconstruction

There are many meteorological records in northern Fennoscandia, but they differ in length. In order to produce a regional average, without the changes in variance that occur when stations are added or removed, six stations were chosen (Figure 1) to provide reasonably even areal coverage and which all extend over the period AD 1890 to AD 2005. The Khibiny data are an updated version of the composite series produced by Kononov et al. (2009). The climate data used for calibration are included with the proxy data at NOAA.

The individual chronologies all correlate most strongly with the temperature of either July or August, but in every case the correlation improves when July and August are combined. Adding June, or taking the average temperature of May to September

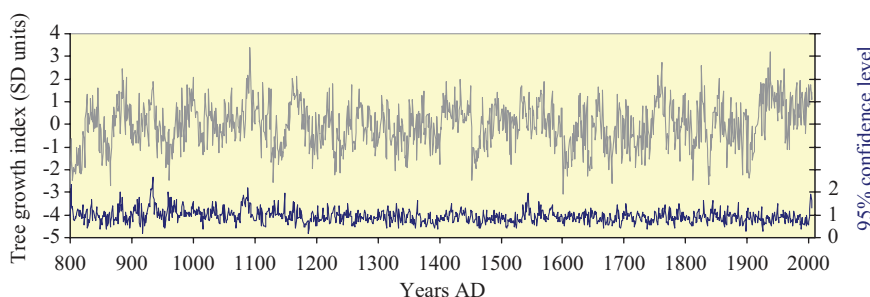


Figure 4. Tree growth index for northern Fennoscandia based on the average of six to nine proxy series with 95% uncertainty values. The growth index values have been normalised over the common period AD 1082 to AD 2005 and the uncertainty values are adjusted by the same factor.

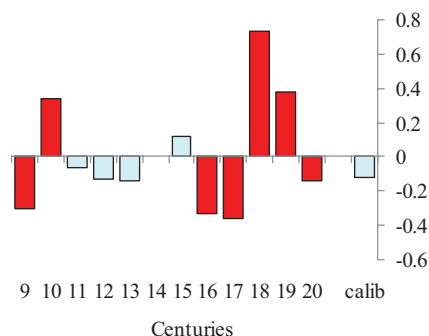


Figure 5. Difference in mean index values (SD units) of Torneträsk and Laanila densities (T-L) for the calibration period (calib: AD 1890 to AD 2005) and for each century. Red (darker) columns are statistically significant (paired *t*-test, $p < 0.05$) (colour figure available online).

gives similar results. When the mean growth index is used, the highest correlation is obtained with the mean temperature of June to August (0.81) but July to August (0.80) and May to September (0.78) give similar results. On the basis of the correlations, the decision about which combination of months to use as a target for climate reconstruction is somewhat arbitrary. Here we use the mean temperature of June to August, on the basis that these are the months when the cambium is active and new cells are being formed (Schmitt et al., 2004; Seo et al., 2011) and for ease of comparison with several other studies that have used the same target for reconstruction (Esper et al., 2012; Gouirand et al., 2008; Tuovinen et al., 2009).

There are several ways in which the nine growth indices could be combined to reconstruct the climate of the past. Multiple regression, for example, with the nine indices as explanatory variables of temperature, could be used to weight (or using a step-wise approach to select and weight) each of the series, and to maximise the amount of variance in summer temperatures explained over the calibration period. However, an underlying assumption of any multiple regression based climate reconstruction method is that the similarity in behaviour of the proxies during the calibration period is a very good indication of the similarity of their behaviour in the past. It is clear from the chronologies that this assumption is not valid. Torneträsk density and Laanila density, for example, are very strongly correlated with JJA temperature (r values of 0.74 and 0.75) and with each other ($r = 0.81$) during the calibration period, so multiple regression will assign one of them a strong weight, but not both, on the basis that they carry approximately the same information. However, the long-term evolution of these two series is not identical. Over the calibration period the two series are so similar that they could have been taken from a single population (difference in means is 0.12 SD units, paired *t*-test: $p = 0.06$), but for seven of the last 12 centuries the difference in mean values is much larger and statistically significant (20th century $p < 0.05$, all others

$p < 0.001$). In fact the only times when the two series are in very close agreement are the calibration period and the 11th to 15th centuries (Figure 5).

An alternative strategy would be to use weighted averaging, where the weight of each series is determined by the amount of variance explained during the calibration period (McCarroll et al., 2003, 2011). In this case all proxies that correlate strongly with climate receive a high weight, irrespective of how highly they correlate with each other. This method ensures that all strong proxies are included, but assumes that the relative strength of the climate signal in the nine proxies remains constant through time, which is difficult to test. The large differences in the correlation matrices for the calibration period and for the remainder of the common period (Table 3) cast some doubt on this assumption. Of the 45 pairs of r -values, 22 are significantly different (*z*-test, $p < 0.05$).

In the case of the nine proxies used here there is little, if anything, to be gained by making the assumptions required for either multiple regression or weighted averaging. The weighted mean series produced by step-wise multiple regression, using the Bayes' information criterion, includes Torneträsk density, Khibiny blue, Forfjorddalen density and Laanila height, weighted in that order, and correlates with mean JJA temperature at 0.84. The mean series produced by weighted averaging correlates with mean JJA temperature at 0.83. Neither of these methods produces correlations that are appreciably or significantly higher than that obtained by simply taking the average of the nine series *z*-scored over the common period ($r = 0.81$, residual standard error 0.66). Similarly, taking the first principal component of the nine series does not add value because it is almost identical to the simple arithmetic mean ($R^2 = 0.99$). On the grounds of parsimony, we conclude that the simple average of the nine growth indices, which invokes the fewest assumptions and still gives a very high correlation with the target climate variable, provides a reasonable predictor of past variations in summer temperature for this region.

The skill of the simple average of the nine *z*-scored series at reconstructing regional average summer (JJA) temperature was tested by splitting the data into equal length calibration (AD 1948 to 2005) and verification (AD 1890–1947) periods and applying the tests recommended by the National Research Council (2007): the squared correlation coefficient (R^2), Reduction of Error (RE) and Coefficient of Efficiency (CE) statistics (Table 4). There is a clear offset in mean JJA temperature between the two periods, so the RE statistic provides a particularly valuable test of the ability of the proxy series to follow a shift in the level of temperature (Wahl and Ammann, 2007). Both RE and CE are positive (0.67 and 0.64) and 72% of the variance in temperature during the verification period is explained. When the calibration and verification periods are reversed, the RE and CE statistics remain strongly positive (0.58 and 0.53) and 56% of the variance in temperature is explained. When regression over the full period AD 1890 to 2005 is used to reconstruct summer temperature, the residuals are not highly autocorrelated (Durbin-Watson statistic = 1.68).

Table 2. Correlation (Pearson's *r*) between the nine proxy series and mean temperature of individual and groups of months. Mean row refers to correlation between the mean chronology and temperature. The meteorological data are the average of six stations (Tromsø, Karesuando, Haparanda, Karasjok, Vardø, Khibiny).

	May	June	July	Aug	Sep	JA	JJA	MJJAS
F-D	0.36	0.39	0.49	0.48	0.21	0.58	0.61	0.61
F-RW	0.16	0.26	0.41	0.28	0.15	0.43	0.44	0.40
T-D	0.40	0.53	0.50	0.63	0.27	0.66	0.74	0.73
T-RW	0.28	0.27	0.60	0.38	0.23	0.61	0.57	0.56
L-D	0.41	0.44	0.58	0.66	0.31	0.73	0.75	0.75
L-RW	0.26	0.22	0.47	0.36	0.16	0.50	0.47	0.46
L-H	0.16	0.28	0.52	0.37	0.12	0.55	0.53	0.46
K-B	0.37	0.36	0.59	0.61	0.26	0.72	0.70	0.68
K-RW	0.21	0.20	0.45	0.36	0.19	0.49	0.46	0.44
Mean	0.40	0.45	0.70	0.64	0.29	0.80	0.81	0.78

Notes:

F: Forfjorddalen; T: Torneträsk; L: Laanila; K: Khibiny; D: density; RW: ring width; H: height increment; B: blue reflectance.

Table 3. Correlation (Pearson's *r*) between the indexed series and the mean chronology (Mean) over both the calibration period and the remainder of the common period.

	F-D	F-RW	T-D	T-RW	L-D	Calibration period AD 1890 to AD 2005				Mean
						L-RW	L-H	K-B	K-RW	
F-D		0.62	0.60	0.42	0.51	0.32	0.41	0.40	0.27	0.69
F-RW	0.50		0.32	0.36	0.34	0.37	0.62	0.17	0.22	0.60
T-D	0.52	0.25		0.65	0.81	0.48	0.41	0.57	0.37	0.80
T-RW	0.24	0.20	0.53		0.68	0.73	0.42	0.46	0.70	0.81
L-D	0.30	0.09	0.52	0.44		0.66	0.55	0.72	0.53	0.89
L-RW	0.03	0.04	0.37	0.54	0.65		0.43	0.36	0.69	0.75
L-H	0.19	0.23	0.24	0.36	0.41	0.45		0.42	0.27	0.69
K-B	0.35	0.15	0.50	0.29	0.57	0.30	0.34		0.45	0.71
K-RW	-0.04	0.09	0.23	0.41	0.42	0.50	0.33	0.36		0.67
Mean	0.54	0.45	0.72	0.70	0.77	0.68	0.62	0.67	0.58	
Rest of common period AD 1082 to AD 1889										

Notes:

Differences that are statistically significant are underlined (z-test for two correlation coefficients, $p < 0.05$).

F: Forfjorddalen; T: Torneträsk; L: Laanila; K: Khibiny; D: density; RW: ring width; H: height increment; B: blue reflectance.

Table 4. Calibration and verification statistics for mean chronologies used in the nested reconstruction.

Series <i>n</i>	Calibration	Verification	R^2	MSE	RE	CE
9	1948–2005	1890–1947	0.72	0.48	0.67	0.64
9	1890–1947	1948–2005	0.56	0.50	0.58	0.53
8	1948–2005	1890–1947	0.72	0.54	0.63	0.59
8	1890–1947	1948–2005	0.59	0.50	0.58	0.54
7	1948–2005	1890–1947	0.67	0.68	0.53	0.49
7	1890–1947	1948–2005	0.58	0.52	0.56	0.51
6	1948–2005	1890–1947	0.64	1.11	0.23	0.16
6	1890–1947	1948–2005	0.54	0.61	0.49	0.43

Notes:

MSE: mean squared error; RE: reduction of error; CE: coefficient of efficiency.

The skill of the reconstruction can be further tested using the long instrumental composite series from Tornedalen (Klingbjer and Moberg, 2003), a border area between Finland and Sweden north of the Gulf of Bothnia, Baltic Sea. This temperature record extends back to 1802, although there is some uncertainty in the summer temperature values prior to 1833, as thermometers at that time were not properly shielded (Böhm et al., 2010). Over the calibration period (AD 1890 to 2005) the correlation between mean JJA temperature and the mean tree growth index is $r = 0.75$. The verification statistics using the period AD 1833 to AD 1889 are very

high and even when the verification period is extended back to AD 1802 the RE and CE values remain strongly positive (Table 5). These results give confidence that the climate reconstruction based on mean tree growth is temporally stable and reliable.

Many previous studies using tree rings to reconstruct past climate have encountered problems with a divergence between the proxy series and temperature data in recent decades (e.g. D'Arrigo et al., 2008). It is notable that in this study there is no evidence for divergence. On the contrary, the correlation between the mean proxy record and summer (JJA) temperature over the final 30

years (AD 1976 to 2005) is the same as the average of all 87 consecutive moving 30 year periods since 1890 ($r = 0.79$). The variability in the strength of the correlation through time is very small (0.84 to 0.72 for all consecutive 30 year periods).

The mean of the z -scored chronologies (annual, non-smoothed data) correlates strongly with gridded mean JJA temperature (AD 1901 to 2005) over a very large area of Fennoscandia and north into Svalbard (Figure 6). The correlation with gridded sea surface temperatures (SST) extends beyond the northern coast of Fennoscandia, and locally strong ($r > 0.5$) positive correlations are also found with SST in the western North Atlantic (AD 1890 to 2005). This pattern, similar to that shown by Rodwell and Folland (2003), suggests that North Atlantic SST influences or may be linked to temperature variability in Northern Fennoscandia during summer.

Given the strong calibration and verification statistics, a nested reconstruction (Meko, 1997) of JJA regional temperature was produced using inverse calibration (using tree growth to predict temperature; Figure 7). A nested approach is required because of the unequal length of the series, ensuring that the calibration for each time period is based only on those series that are available for reconstruction. There are four steps in the nested reconstruction and in each case the RE and CE statistics are positive (Table 4).

Uncertainty of regression-based climate reconstructions is often presented simply as two standard errors (2SE) of the prediction, which in this case is $\pm 1.32^\circ\text{C}$ using nine series, rising to $\pm 1.48^\circ\text{C}$ before AD 821 when the number of series is six. However, this simple measure of uncertainty is always an underestimate in palaeoclimate reconstructions as it ignores the uncertainty in the mean values upon which the reconstruction is based. In this case the uncertainty in the mean annual tree growth index (effectively the coherence between the series) can also be incorporated simply by applying the same nested reconstruction equations used

Table 5. Calibration and verification statistics using the long instrumental temperature record from Tornedal.

Calibration	Verification	R^2	MSE	RE	CE
1890–2005	1833–1889	0.61	0.47	0.70	0.60
1890–2005	1802–1889	0.47	0.66	0.57	0.47

Notes:

MSE: mean squared error; RE: reduction of error; CE: coefficient of efficiency.

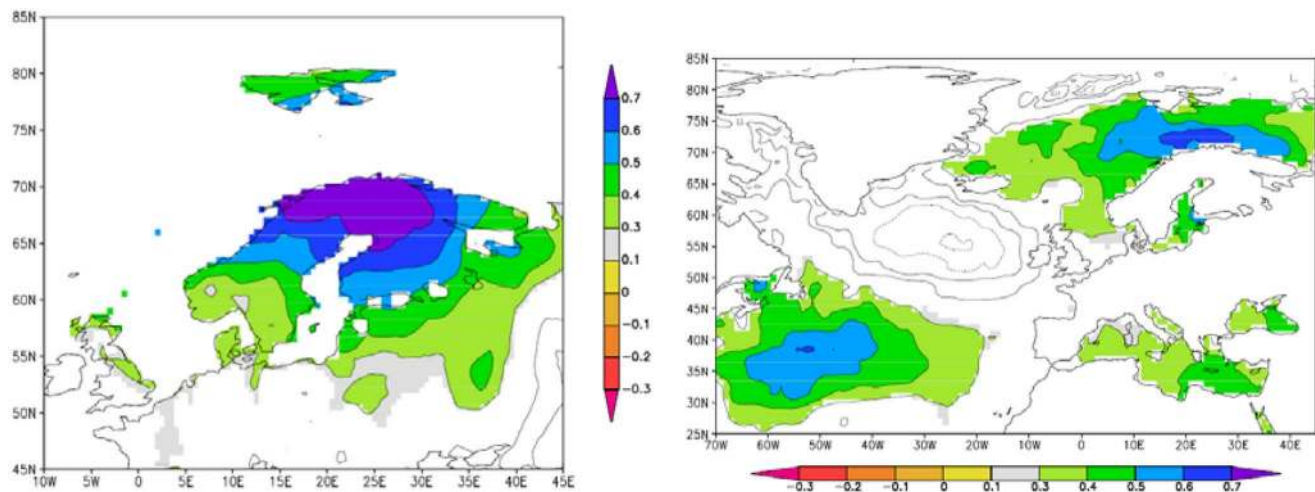


Figure 6. Spatial field correlations between the mean tree growth index and gridded summer (JJA) temperature (CRU TS3, 1901–2005) and between the mean tree growth index and gridded sea surface temperature (HadISST1, 1890–2005). Coloured bars show correlation coefficients (Pearson's r ; $p < 0.01$). Maps were produced using KNMI Climate Explorer (<http://climexp.knmi.nl/>; van Oldenborgh et al., 2004).

for the mean curve and applying them to the upper and lower 95% confidence limits. This measure of uncertainty can then be combined with the 2SE of the regression using Gaussian error propagation (square root of the sum of the two squared errors). This combined error will overestimate the true uncertainty because the two errors are not fully independent; the uncertainty in estimation of mean growth during the calibration period must contribute to the unexplained variance and therefore to the calibration error. Moreover, these uncertainty estimates apply to the annual values only and the uncertainty of smoothed series or of decadal or longer period mean estimates will be much smaller because the uncertainty in mean tree growth over longer periods is less. A more complete treatment of uncertainty in proxy-based reconstructions will be attempted elsewhere, but Figures 7 and 8 suffice to demonstrate the temporal changes in uncertainty that are often neglected.

Using the uncertainty based on regression alone is clearly unrealistic (Figure 7). Although the regression error is, on average, the higher of the two, there are many years and groups of years where the uncertainty resulting from poor coherence between the proxies is much larger. Given that the highest replication within each series occurs in the 20th century, we would expect uncertainty to increase back in time, and although that is true the magnitude of increase is actually very small. The mean annual combined error for the 20th century is $\pm 1.71^\circ\text{C}$, but for the previous seven centuries it never rises above 1.78°C (16th century), so the increase in uncertainty is less than 4.5% (Figure 8). For the 12th and 11th centuries the mean annual uncertainty is 6% and 12% higher than the 20th century ($\pm 1.81^\circ\text{C}$ and $\pm 1.91^\circ\text{C}$) entirely as a result of greater uncertainty in the estimate of mean growth, reflecting less coherence between the proxies. The largest mean annual uncertainty occurs in the 10th century ($\pm 1.97^\circ\text{C}$, 16% higher than 20th century), reflecting both less coherence and a drop in the number of series available. Uncertainty for the 9th century is somewhat lower, despite the loss of series and tree replication ($\pm 1.81^\circ\text{C}$, 6% higher than 20th century), reflecting higher interseries coherence (Figure 8).

When inverse calibration is used to reconstruct past temperatures, there is always a loss of variance in the reconstruction that is proportional to the amount of unexplained variance during the calibration period (Birks, 1995; Esper et al., 2005; Moberg and Brattström, 2011; Robertson et al., 1999). Even though the correlation between the mean growth index and regional mean JJA temperature is unusually high ($r = 0.81$), there is still an appreciable loss of variance. The total range of measured JJA temperature

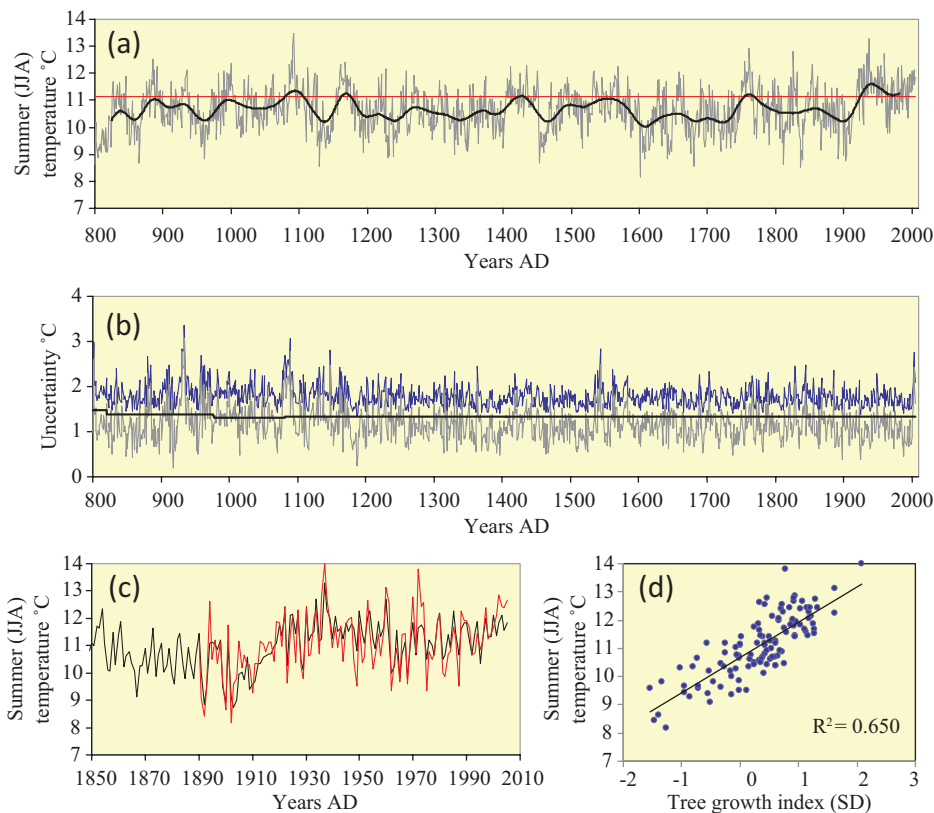


Figure 7. (a) Nested reconstruction of summer (JJA) temperature based on regression. Grey (fine) line is annual values and the bold line is a 50 yr Gaussian filter. Red horizontal line is the mean (reconstructed) summer temperature of the 20th century. (b) Uncertainty in annual summer temperature estimates (\pm 95%) based on coherence (lower grey line) between the proxy series (95% confidence limit around the mean tree growth index), two standard errors of the regression equations in the nested reconstruction (stepped black line) and a combination of the two using Gaussian error propagation (upper blue/darker line). (c) Expanded modern portion showing fit with regional mean measured summer temperature (red). (d) Scatter plot showing the correlation between mean tree growth index and measured summer (JJA) temperature based on all nine chronologies (colour figure available online).

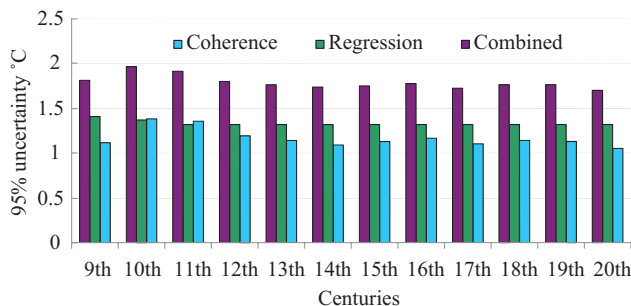


Figure 8. Uncertainty in the average annual summer temperature estimates (\pm 95%) for each century based on coherence between the proxy series (95% confidence limit around the mean tree growth index), two standard errors of the regression equations in the nested reconstruction and a combination of the two using Gaussian error propagation. The combined error is an overestimate of true uncertainty because the two errors are not independent.

values over the instrumental period AD 1890 to 2005 is 5.8°C, but the reconstructed range over the same period is only 4.6°C; a reduction of almost 22%. One way to avoid this bias is to ‘scale’ the proxy series so that it has the same mean and variance as the climatic target data over the calibration period. This common procedure is somewhat problematic, because the tree growth series being scaled to temperature contains both signal and noise, and a noisy climate record should not have the same variance as an instrumental series. Nevertheless, the magnitude of climate variability in the scaled reconstruction is likely to be closer to the true

range than that produced using inverse calibration, which is certainly an underestimate, despite the very strong calibration and verification statistics. In this case (Figure 9) the scaled reconstruction produces a range of 5.7°C over the instrumental period, a loss of only 3%. The scaled reconstruction is therefore used in the discussion of absolute changes in temperature and of the impacts of natural forcing.

It should be stressed that the scaled reconstruction lies entirely within the 95% uncertainty bounds defined using the combined uncertainty resulting from regression and coherence. The nested reconstruction based on regression and the scaled reconstruction can thus be viewed as two ‘best estimate’ curves that provide rather different information but which for these data sets both lie within the same envelope of uncertainty. The former minimises the mean squared error over the calibration period but underestimates the magnitude of variability in the past, whereas the latter probably gives a more realistic picture of the magnitude of past climate change at the expense of inflating the error.

Since the reconstructions of JJA temperature are simply a scaling of the mean tree growth record discussed earlier, the conclusions are unaffected. The 20th century experienced the warmest summers and the 17th century the coldest. The warmest pre-industrial century was the 11th, and since the uncertainty of the climate reconstruction cannot be less than that of the mean growth curve on which it is based, it is inevitable that the reconstructed mean summer temperatures of the 20th and 11th centuries are not significantly different. The warmest summer in the regression-based reconstruction is AD 1092 (13.47 \pm 1.32°C), followed by AD 1937 (reconstructed mean JJA temperature 13.29 \pm 1.32°C, measured temperature 14.0°C). If the scaled reconstruction is used the

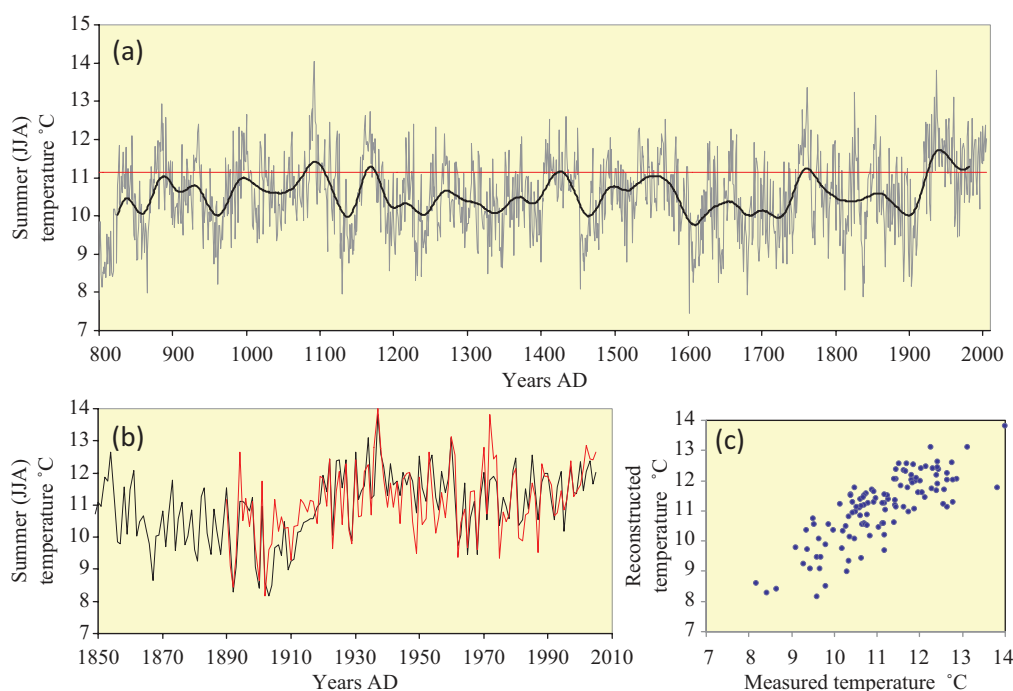


Figure 9. (a) Nested reconstruction of summer (JJA) temperature based on variance scaling. Grey (fine) line is annual values and the bold line is a 50 yr Gaussian filter. Red horizontal line is the mean (measured) summer temperature of the 20th century. (b) Expanded modern portion showing fit with regional mean measured summer temperature (red/shorter). (c) Scatter plot showing the relationship between measured and reconstructed mean summer temperatures (colour figure available online).

values for AD 1937 and AD 1092 are 13.82°C and 14.04°C, respectively. The coldest summer occurred in AD 1601 ($8.16 \pm 1.33^\circ\text{C}$ by regression, 7.46°C by scaling).

Natural forcing

When the summer temperature reconstruction is compared with estimates of natural climate forcing (Figure 10) the impact of volcanism (Gao et al., 2008) is clear. There are particularly abrupt growth suppressions, and inferred drops in summer temperature, associated with known eruptions (Siebert et al., 2010) at AD 1227, AD 1258, AD 1452, AD 1600, AD 1641, AD 1831 and AD 1963. Where there are two large eruptions in close succession the impact on summer temperatures is particularly marked. The clearest example occurs in the mid-15th century, with eruptions in AD 1452 (Kuwae caldera, probably the greatest sulphuric acid aerosol producer in the last seven centuries; Gao et al., 2006; Witter and Self, 2007) and AD 1459 resulting in an abrupt drop in summer temperature of about 4°C. Temperatures recover by AD 1470 but are again depressed by eruptions in AD 1474, AD 1476 and AD 1480. The pairs of eruptions in AD 1809 and AD 1815 and in AD 1831 and AD 1835 are also apparent in the temperature reconstruction. Some more prolonged cold periods that seem to be associated with periods of repeated, though not necessarily very large eruptions are also apparent, including AD 1040 to AD 1060, AD 1167 to AD 1213 and AD 1693 to AD 1738. Although the impact of most single eruptions is short-lived, it is clear that where eruptions come in pairs or in multiples, the effects can last beyond the common three-year lifetime of volcanic aerosols (Oman et al., 2005). A cumulative impact of successive eruptions and a delayed recovery requires some positive feedback. Increased snow cover and sea ice extent, and the attendant increases in surface albedo and changes in heat distribution and atmospheric circulation, seem likely candidates (Miller et al., 2012; Wanamaker et al., 2012). A comparison with chronologies from sites not directly affected by sea-ice conditions (e.g. mid and high latitudes in the Southern Hemisphere) could help disentangle the relevant mechanisms.

The relationship between summer temperatures and solar forcing is much less clear (Figure 10), especially prior to AD 1600. The Oort minimum of the 11th century was not associated with cold summers. The Spörer minimum of the 15th century includes very cold summers, and in a lower resolution record it would be difficult to separate the effects of volcanism and solar forcing during this period. However, in this annually resolved reconstruction it is very clear that the low summer temperatures are caused by an abrupt response to volcanism, and a recovery that is delayed by further eruptions. The gap in volcanism during the Spörer minimum, in the AD 1490s, is associated with higher than average summer temperatures (Figure 10). The coldest summers in the Wolf, Maunder and Dalton minima are also associated with volcanism. Over the whole 1200-year reconstruction, most of the cold decades fall outside of the solar minima, including AD 858 to AD 867, AD 956 to AD 965, AD 1137 to AD 1146, AD 1238 to AD 1247, AD 1601 to AD 1610, AD 1832 to AD 1841 and AD 1900 to AD 1909. The mediaeval solar maximum, approximately AD 1100 to AD 1250, includes three prolonged periods of cool summers and just two short intervals of relative warmth. The warmest pre-industrial century is the 11th, which pre-dates the solar maximum and includes the Oort minimum. The correlation between reconstructed summer temperature (nested regression) and solar forcing is extremely weak ($r = 0.07$), so less than 0.5% of the variance is explained. The evidence does not appear to support a strong link between solar forcing and summer temperatures in northern Fennoscandia. The structure of the volcanic forcing data set precludes a similar statistical comparison.

This record is not long enough to provide a reliable estimate of the impact of orbital forcing, but it is interesting that over the last millennium, and removing the 20th century, the scaled reconstruction yields a decline of $0.31^\circ\text{C}/1000$ years, which is exactly the same as that obtained by Esper et al. (2012) for northern Fennoscandia over the last two millennia, also excluding the 20th century. There is thus no reason to suggest that the reconstructions presented here underestimate the long-term cooling effect of orbital forcing.

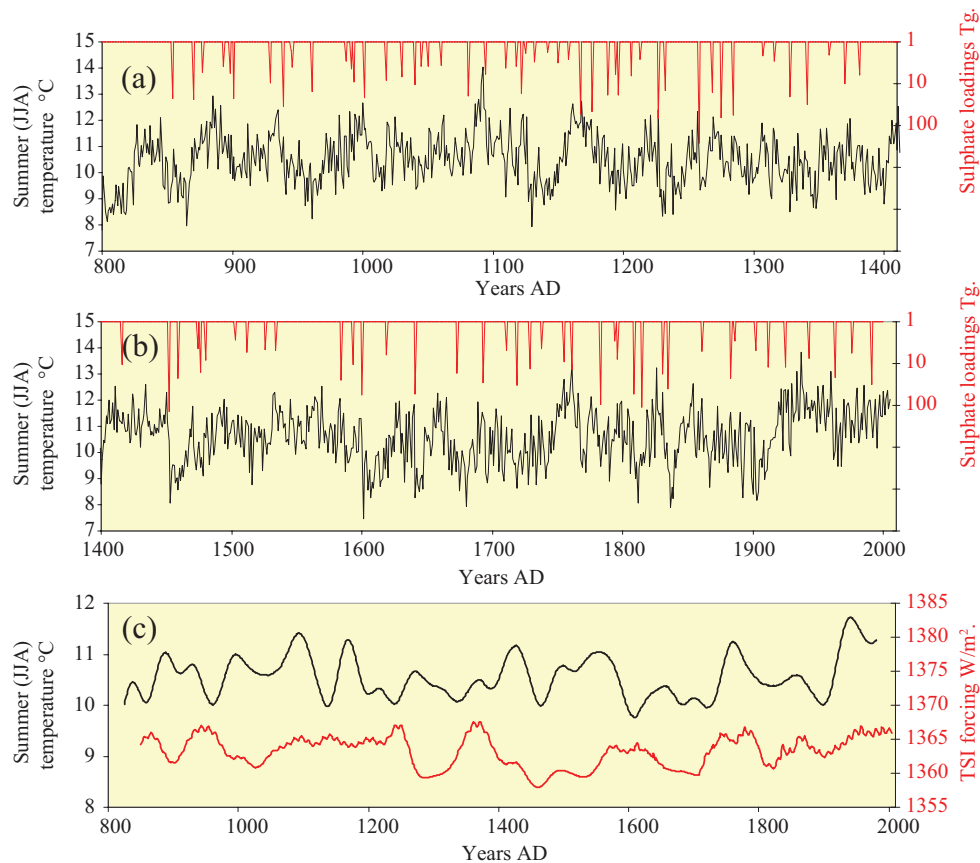


Figure 10. The scaled summer temperature reconstruction compared with (a and b) the global volcanic sulphate loadings series of Gao et al. (2008), and (c) smoothed with a 100-year Gaussian filter for comparison with the total solar irradiance reconstruction (red/lower line) of Shapiro et al. (2011) (colour figure available online).

Discussion and conclusions

The reconstructions presented here, based on simple linear regression and variance scaling of the mean tree growth index with a regional mean value for JJA temperature, rely on very simple methods, and thus make very few assumptions. Nevertheless, the correlation with regional mean summer temperature is very high ($r = 0.81$) and verification tests using split periods and using the longest early instrumental data from the region suggest that the reconstructions are reliable. The results suggest that the 20th century was the warmest of the last 1200 years, but that it was not significantly different from the 11th century. The coldest century was the 17th.

The approach taken here works particularly well because it includes a mix of proxies, includes data from several well-separated sites, and represents a very large sample. It has been argued elsewhere that a multiproxy approach to climate reconstruction is advantageous because different proxies tend to have different sources of error, so combining them accentuates the climate signal whilst cancelling noise (Gagen et al., 2006; McCarroll et al., 2003, 2011). Including several well-separated sites is important because all tree stands are subject to disturbance events resulting in local changes in growth that can easily be misinterpreted as climatic. These can include very local events such as wind-throw, resulting in reduced competition and growth release (mimicking warming) but also events that can impact over a wider area, including human influence and fire (Gunnarson et al., 2012).

Even in remote locations such as the northern pine forest limit of Europe the impact of humans cannot be completely discounted (Josefsson et al., 2009, 2010). The whole region has a very long history of low-intensity land use by the indigenous Sami people, who used the forests for winter reindeer grazing and also

harvested wood and wood products, including pine bark (Östlund et al., 2003). Gunnarson et al. (2012) have demonstrated that the impacts of such low-intensity activities are measurable in both tree ring widths and densities and will influence climate reconstructions based upon them. There is clear evidence of Sami activity at Forfjordalen in Norway and at Torneträsk in Sweden, and there is no reason to suspect that the other sites were not also utilised. It is unlikely, however, that human impacts will have resulted in identical or synchronous changes at four such distant sites. Averaging is, therefore, likely to dampen any cultural impacts, whilst retaining the common signal of regional climate change. Similarly, fire is an important component of the boreal forest ecosystem and past forest fires will have a significant impact on surviving trees, resulting in growth changes which may be misinterpreted as being climatically driven. Even taking the exceptionally long fire recurrence interval of about 350 years proposed by Wallenius et al. (2010) on the basis of fire scars on dated pine trees in northern Finland, and supported by longer-term records from charcoal in lake sediments (Carcaillet et al., 2007) we would expect several fires at each site over the course of the last 1200 years. Although some boreal forest fires can cover very large areas ($> 10,000$ ha), most are much smaller and perhaps caused by humans (Wallenius et al., 2010). Combining data from several widely spaced sites is again likely to cancel out the disturbance effects of fires and enhance the regional climate signal.

Combining data from sites over a long transect also has the advantage of producing a reconstruction that is representative of the climate of a very large area. We find high ($r > 0.5$) correlations with the gridded summer air temperature across the whole of Finland and across central and northern Sweden and Norway, as well as significant ($r > 0.3$, $p < 0.01$) correlations across the whole of

Fennoscandia, extending north across Svalbard and south into Denmark. Correlation with gridded sea surface temperatures is strong enough to capture the teleconnection between Norwegian coastal waters and the western North Atlantic (Figure 6).

Reconstructions of past temperature that represent such large regions are particularly suited to testing the ability of General Circulation Models (GCMs) to reconstruct the climate of the past. Such tests are the most promising way to reduce uncertainty in the sensitivity of climate to forcing and thus of the likely evolution of climate, at a variety of spatial scales, under enhanced greenhouse conditions (Edwards et al., 2007; Knutti and Hegerl, 2008; McCarroll, 2010). The grid cells in GCMs, particularly if they are run over a long period or as part of a perturbed physics ensemble (Rowlands et al., 2012), tend to be very large, and adjacent cells cannot be considered as independent, so it is problematic to test such models using climate reconstructions that are specific to single sites.

A great advantage of using the arithmetic average of the nine normalised chronologies, rather than a more complicated approach to combining them, is that the mean value can be furnished with uncertainty estimates that are simple and transparent. Here we have used the 95% confidence limits, which for nine chronologies (8 degrees of freedom) is 2.31 standard errors (standard deviation divided by square root of sample size). The higher and lower uncertainty bounds for the mean tree growth index are translated into temperature units using the same nested regression method applied to the mean series and then combined with the regression uncertainty (2 standard errors of the prediction) using Gaussian error propagation. This procedure is not beyond critique, but it does serve to quantify the changes in uncertainty over time that reflects changes in the degree of coherence, or agreement, between the proxy series. This is certainly better than the common method of relying solely upon the uncertainty in the regression procedure, particularly where there are large differences in replication through time (which is almost always the case). Rather than focusing on the values of the uncertainty estimates, which are very likely to be an inflated measure of the real uncertainty in the annual temperature reconstruction, a profitable approach is to simply compare uncertainty in the past with that for the 20th century, when we are certain that the fit between the mean growth index and measured summer temperature is excellent. The results of such an analysis are surprisingly good, suggesting that errors over the last millennium are not much larger (< 4% to 12%) than during the 20th century.

Esper et al. (2012) compared temperature reconstructions across northern Fennoscandia, demonstrating that although temperature variations are often synchronous, the offset in absolute values of the reconstructions is sometimes large. They conclude that their findings 'demonstrate our poor understanding of the absolute temperature variance in a region where high-resolution proxy coverage is denser than in any other area of the world'. The nine series included in the reconstruction presented here also show offsets, particularly in the early part of the record when replication is lower, but by combining them we have produced a mean series that is stronger than any individual record and which has an uncertainty estimate that includes information on changes in the offset in absolute values over time. Comparing the size of the uncertainty in the past with that in the 20th century suggests that the estimated summer temperatures of the past are not as insecure as Esper et al. (2012) suggest. Adding replication or new series would reduce the uncertainty even further. Careful, expert development of robust, regionally representative palaeoclimate reconstructions are an essential first step in this effort, but there is likely much more to be gained across northern Fennoscandia, and other proxy-rich regions, from further inclusive scientific collaborations of this kind than can be realised from an individual or competitive approach.

The evidence presented here suggests that, superimposed on the slow (0.31°C/1000 yr) cooling in response to orbital forcing, the dominant control on pre-industrial summer temperatures in the far north of Europe was explosive volcanic eruptions. However, the link between sulphate loadings recorded in the polar ice cores and the temperature response is clearly non-linear, as can be expected from the dynamics of volcanic aerosols (Timmreck et al., 2009). Sulphate loadings of individual eruptions do not appear to be a good predictor of the magnitude of associated climate (or tree) response, and pairs or multiple eruptions in quick succession have a much greater and more sustained impact than a single larger eruption. The largest tropical eruption of the last millennium, in AD 1258/AD 1259, for example, had less apparent impact than the closely spaced eruptions of AD 1452, AD 1474, AD 1476 and AD 1480 and the last of three closely spaced eruptions results in the coldest year of the sequence in AD 1601. It is clear from the climate reconstructions that recovery following individual eruptions is very rapid, but that recovery from pairs or multiple eruptions can extend well beyond the three year lifetime of volcanic aerosols (Oman et al., 2005). This implies some positive feedback in the climate system.

The results presented here agree extremely well with those produced by Miller et al. (2012) based on radiocarbon dating of moss recently exposed by the melting of Arctic plateau ice fields and thus indicative of abrupt summer cooling resulting in persistent snowline depression and ice advance. Miller et al. (2012) find distinct peaks in their dates between AD 1275 and AD 1300 and between AD 1430 and AD 1455 and attribute these to periods with repeated explosive eruptions resulting in abrupt summer cooling. In our tree ring records the individual eruptions are clearly identifiable. As well as the albedo feedback generated by increased ice cover on both sea and land, Miller et al. (2012) suggest that increased southward sea ice export results in a weakening of the Atlantic meridional overturning circulation and thus in northward heat transport in the North Atlantic. This is supported by the modelling work of Zhong et al. (2011) who showed that reduced basal sea ice melting could result in an expanded sea ice state that persists for decades after the final eruption. Further support for a marine influence in maintaining cold conditions during the 'Little Ice Age' comes from the radiocarbon dating of annually banded shells north of Iceland, which reveals changes in local radiocarbon reservoir age offsets, and thus relative dominance of Arctic (older) and Atlantic (younger) water masses (Wanamaker et al., 2012).

In contrast, we find no clear link between summer temperature and solar forcing. The magnitude of past changes in solar irradiance remains very uncertain (Lean, 2005; Shapiro et al., 2011) but the pattern of temporal changes over the last millennium is generally agreed. Visual comparison of the smoothed temperature reconstruction and a solar forcing curve suggests some correspondence over the last few centuries, but there is a serious problem of conflation between the volcanic and solar forcings at this time (Breitenmoser et al., 2012). The Maunder Minimum of the 17th century, for example, is also a time of enhanced volcanism. The clearest example, however, is the Spörer minimum of the 15th century, which includes a cold period in the smoothed temperature reconstruction which at annual resolution is clearly an abrupt response to a pair of volcanic eruptions, resulting in an immediate 4°C drop in summer temperature and a recovery that is delayed for decades by repeated eruptions. Many comparisons between solar forcing and climate reconstructions are based on low-resolution proxies, derived from lake, peat or marine sediments, where there is usually considerable uncertainty in the dating. In many cases the possible impact of large volcanic eruptions, and associated feedbacks, are not even considered. On the basis of our results we would urge greater caution in such comparisons because a false or exaggerated connection between solar forcing

and past climate has important implications for our understanding of recent climate change and future predictions (Gray et al., 2010). If a very small influence of solar forcing in the past, as implied by our results for Northern Fennoscandia, is confirmed for other sites around the world, the response to greenhouse gas emissions would remain the only major external factor responsible for the observed 20th century global warming.

Acknowledgements

Special thanks to Professor Sheila Hicks for constantly reminding us of the benefits of collaboration over competition.

Funding

This work was funded by the European Union FP6 project Millennium 017008 and we thank our many friends within and beyond the project for helpful discussion.

References

- Bergsten U, Lindeberg J, Rindby A et al. (2001) Batch measurements of wood density on intact or prepared drill cores using x-ray microdensitometry. *Wood Sciences and Technology* 35: 435–452.
- Birks HJB (1995) Quantitative palaeoenvironmental reconstructions. In: Maddy D and Brew JS (eds) *Statistical Analysis of Quaternary Science Data, Technical Guide 5*. Cambridge: Quaternary Research Association, pp. 161–254.
- Böhm R, Jones PD, Hiebl J et al. (2010) The early instrumental warm-bias: A solution for long central European temperature series 1760–2007. *Climatic Change* 101: 41–67.
- Breitenmoser P, Beer J, Broennimann S et al. (2012) Solar and volcanic fingerprints in tree-ring chronologies over the past 2000 years. *Palaeogeography Palaeoclimatology Palaeoecology* 313: 127–139.
- Briffa KR, Bartholin TS, Eckstein D et al. (1990) A 1,400-year tree-ring record of summer temperatures in Fennoscandia. *Nature* 346: 434–439.
- Campbell R, McCarroll D, Loader NJ et al. (2007) Blue reflectance in *Pinus sylvestris*: Application, validation and climatic sensitivity of a new palaeoclimate proxy for tree ring research. *The Holocene* 17: 821–828.
- Campbell R, McCarroll D, Robertson I et al. (2011) Blue intensity in *Pinus sylvestris* tree-rings: A manual for a new palaeoclimate proxy. *Tree Ring Research* 67: 127–134.
- Carcaillet C, Bergman I, Delorme S et al. (2007) Long-term fire frequency not linked to prehistoric occupations in northern Swedish boreal forest. *Ecology* 88: 465–477.
- D'Arrigo R, Wilson R, Liepert B et al. (2008) On the 'divergence problem' in northern forests: A review of the tree-ring evidence and possible causes. *Global and Planetary Change* 60: 289–305.
- Edwards TL, Crucifix M and Harrison SP (2007) Using the past to constrain the future: How the palaeorecord can improve estimates of global warming. *Progress in Physical Geography* 31: 481–500.
- Eronen M, Zetterberg P, Briffa KR et al. (2002) The supra-long Scots pine tree-ring record for Finnish Lapland: Part 1, chronology construction and initial inferences. *The Holocene* 12: 673–680.
- Esper J, Cook ER, Krusic PJ et al. (2003) Tests of the RCS method for preserving low-frequency variability in long tree-ring chronologies. *Tree-Ring Research* 59: 81–98.
- Esper J, Frank DC, Timonen M et al. (2012) Orbital forcing of tree ring data. *Nature Climate Change* DOI: 10.1038/nclimate1589.
- Esper J, Frank DC, Wilson RJS et al. (2005) Effect of scaling and regression on reconstructed temperature amplitude for the past millennium. *Geophysical Research Letters* 32: L0771. doi: 10.1029/2004GL0236.
- Gagen M, McCarroll D and Edouard JL (2006) Combining ring width, density and stable carbon isotope proxies to enhance the climate signal in tree-rings: An example from the southern French Alps. *Climatic Change* 78: 363–379.
- Gagen MH, McCarroll D, Loader NJ et al. (2007) Exorcising the 'segment length curse': Summer temperature reconstruction since AD 1640 using non de-trended stable carbon isotope ratios from pine trees in northern Finland. *The Holocene* 17: 433–444.
- Gao CC, Robock A and Ammann C (2008) Volcanic forcing of climate over the past 1500 years: An improved ice core-based index for climate models. *Journal of Geophysical Research-Atmospheres* 113: D09103.
- Gao CC, Robock A, Self S et al. (2006) The 1452 or 1453 AD Kuwae eruption signal derived from multiple ice core records: Greatest volcanic sulfate event of the past 700 years. *Journal of Geophysical Research-Atmospheres* 111: D15105.
- Gouirand I, Linderholm HW, Moberg A et al. (2008) On the spatiotemporal characteristics of Fennoscandian tree-ring based summer temperature reconstructions. *Theoretical and Applied Climatology* 91: 1–25.
- Gray LJ, Beer J, Geller M et al. (2010) Solar influences on climate. *Reviews of Geophysics* 48: 53.
- Grudd H (2008) Torneträsk tree-ring width and density AD 500–2004: A test of climatic sensitivity and a new 1500-year reconstruction of north Fennoscandian summers. *Climate Dynamics* 31: 843–857.
- Grudd H, Briffa KR, Karlén W et al. (2002) 7400-year tree-ring chronology in northern Swedish Lapland: Natural climatic variability expressed on annual to millennial timescales. *The Holocene* 12: 657–665.
- Gunnarson BE and Linderholm HW (2002) Low-frequency summer temperature variations in central Sweden since the 10th century inferred from tree rings. *The Holocene* 12: 667–671.
- Gunnarson BE, Josefsson T, Linderholm HW et al. (2012) Legacies of pre-industrial land use can bias modern tree-ring climate calibrations. *Climate Research* 53: 63–76.
- Gunnarson BE, Linderholm H and Moberg A (2011) Improving a tree-ring reconstruction from west-central Scandinavia: 900 years of warm-season temperatures. *Climate Dynamics* 36: 97–108.
- Helama S, Lindholm M, Timonen M et al. (2002) The supra-long Scots pine tree-ring record for Finnish Lapland: Part 2, interannual to centennial variability in summer temperatures for 7500 years. *The Holocene* 12: 681–687.
- Hughes MK (2002) Dendrochronology in climatology – The state of the art. *Dendrochronologia* 20: 95–116.
- Intergovernmental Panel on Climate Change (2007) *Climate Change 2007: The Physical Science Basis*. Contribution of Working Group I to the Fourth Assessment Report of the IPCC (Solomon S, Qin M, Manning Z et al. (eds.)) Cambridge and New York: Cambridge University Press, 996 pp.
- Jones PD, Briffa KR, Osborn TJ et al. (2009) High-resolution palaeoclimatology of the last millennium: A review of current status and future prospects. *The Holocene* 19: 3–49.
- Josefsson T, Gunnarson BE, Liedgren L et al. (2010) Historical human influence on forest composition and structure in boreal Fennoscandia. *Canadian Journal of Forest Research* 40: 872–884.
- Josefsson T, Hörnberg G and Östlund L (2009) Long-term human impact and vegetation changes in a boreal forest reserve: Implications for the use of protected areas as ecological references. *Ecosystems* 12: 1017–1036.
- Kirchhefer AJ (2001) Reconstructions of summer temperatures from tree-rings of Scots pine (*Pinus sylvestris* L.) in coastal northern Norway. *The Holocene* 11: 41–52.
- Klingbjör P and Moberg A (2003) A composite monthly temperature record from Tornedalen in Northern Sweden, 1802–2002. *International Journal of Climatology* 23: 1465–1494.
- Knutti R and Hegerl GC (2008) The equilibrium sensitivity of the Earth's temperature to radiation changes. *Nature Geoscience* 1: 735–743.
- Kononov YM, Friedrich M and Boettger T (2009) Regional summer temperature reconstruction in the Khibiny Low Mountains (Kola Peninsula, NW Russia) by means of tree-ring width during the last four centuries. *Arctic Antarctic and Alpine Research* 41: 460–468.
- Lean J (2005) Living with a variable sun. *Physics Today* 58: 32–38.
- Linderholm HW, Björklund JA, Seftigen K et al. (2010) Dendroclimatology in Fennoscandia – From past accomplishments to future potential. *Climate of the Past* 6: 93–114.
- Lindholm M, Jalkanen R, Salminen H et al. (2011) The height-increment record of summer temperature extended over the last millennium in Fennoscandia. *The Holocene* 21: 319–326.
- Lindholm M, Ogurtsov M, Aalto T et al. (2009) A summer temperature proxy from height increment of Scots pine since 1561 at the northern timberline in Fennoscandia. *The Holocene* 19: 1131–1138.
- Loader NJ, Young GHF, Grudd H. (2012) Stable carbon isotopes from Torneträsk, northern Sweden provide a millennial length reconstruction of summer sunshine and its relationship to Arctic circulation. *Quaternary Science Reviews* 62: 97–113. <http://dx.doi.org/10.1016/j.quascirev.2012.11.014>.
- McCarroll D (2010) Future climate change and the British Quaternary research community. *Quaternary Science Reviews* 29: 1661–1672.
- McCarroll D, Jalkanen R, Hicks S et al. (2003) Multi-proxy dendroclimatology: A pilot study in northern Finland. *The Holocene* 13: 829–838.
- McCarroll D, Pettigrew E, Luckman A et al. (2002) Blue reflectance provides a surrogate for latewood density of high-latitude pine tree rings. *Arctic Antarctic and Alpine Research* 34: 450–453.
- McCarroll D, Tuovinen M, Campbell R et al. (2011) A critical evaluation of multi-proxy dendroclimatology in northern Finland. *Journal of Quaternary Science* 26: 7–14.

- Mann ME, Bradley RS and Hughes MK (1999) Northern hemisphere temperatures during the past millennium: Inferences, uncertainties, and limitations. *Geophysical Research Letters* 26: 759–762.
- Meko DM (1997) Dendroclimatic reconstruction with time varying subsets of tree indices. *Journal of Climate* 10: 687–696.
- Melvin T, Grudd H and Briffa KR (2012) Potential bias in ‘updating’ tree-ring chronologies using regional curve standardisation: Re-processing 1500 years of Torneträsk density and ring-width data. *The Holocene* DOI: 10.1177/0959683612460791.
- Miller GH, Geirsdottir A, Zhong YF et al. (2012) Abrupt onset of the Little Ice Age triggered by volcanism and sustained by sea-ice/ocean feedbacks. *Geophysical Research Letters* 39: L02708.
- Moberg A and Brattström G (2011) Prediction intervals for climate reconstructions with autocorrelated error noise – An analysis of ordinary least squares and measurement error methods. *Palaeogeography Palaeoclimatology Palaeoecology* 308: 313–329.
- National Research Council (2007) *Surface Temperature Reconstructions for the Last 2,000 Years*. Washington DC: The National Academies Press.
- Oman L, Robock A, Stenchikov G et al. (2005) Climatic response to high latitude volcanic eruptions. *Journal of Geophysical Research* 110: D13103.
- Östlund L, Ericsson TS, Zackrisson O et al. (2003) Traces of past Sami forest use: An ecological study of culturally modified trees and earlier land use within a boreal forest reserve. *Scandinavian Journal of Forest Research* 18: 78–89.
- Robertson I, Lucy D, Baxter L et al. (1999) A kernel-based Bayesian approach to climatic reconstruction. *The Holocene* 9: 495–500.
- Rodwell MJ and Folland CK (2003) Atlantic air–sea interaction and model validation. *Annals of Geophysics* 46: 47–56.
- Rowlands DJ, Frame DJ, Ackerley D et al. (2012) Broad range of 2050 warming from an observationally constrained large climate model ensemble. *Nature Geoscience* 5: 256–260.
- Salminen H and Jalkanen R (2005) Modelling the effect of temperature on height increment of Scots pine at high latitudes. *Silva Fennica* 39: 497–508.
- Schmitt U, Jalkanen R and Eckstein D (2004) Cambium dynamics of *Pinus sylvestris* and *Betula* spp. in the northern boreal forest in Finland. *Silva Fennica* 38: 167–178.
- Seo J-W, Eckstein D, Jalkanen R et al. (2011) Climatic control of intra- and inter-annual wood-formation dynamics of Scots pine in northern Finland. *Environmental and Experimental Botany* 72: 422–431.
- Schweingruber FH. (1988) *Tree Rings: Basics and Applications of Dendrochronology*. Dordrecht: Kluwer Academic Publishers.
- Shapiro AI, Schmutz W, Rozanov E et al. (2011) A new approach to the long-term reconstruction of the solar irradiance leads to large historical solar forcing. *Astronomy & Astrophysics* 529: A67.
- Siebert L, Simkin T and Kimberly P (2010) *Volcanoes of the World, 3rd Edition*. Berkeley: University of California Press, 568 pp. Available at: <http://www.volcano.si.edu/world/>
- Timmreck C, Lorenz SJ, Crowley TJ et al. (2009) Limited temperature response to the very large AD 1258 volcanic eruption. *Geophysical Research Letters* 36: L21708, doi:10.1029/2009GL040083.
- Tuovinen M, McCarroll D, Grudd H et al. (2009) Spatial and temporal stability of the climatic signal in northern Fennoscandian pine tree ring width and maximum density. *Boreas* 38: 1–12.
- van Oldenborgh GJ, Balmaseda MA, Ferranti L et al. (2004) Evaluation of atmospheric fields from the ECMWF seasonal forecasts over a 15 year period. *Journal of Climate* 16: 2970–2989.
- Wahl ER and Ammann CM (2007) Robustness of the Mann, Bradley, Hughes reconstruction of Northern Hemisphere surface temperatures: Examination of criticisms based on the nature and processing of proxy climate evidence. *Climatic Change* 85: 33–69.
- Wallenius TH, Kauhanen H, Herva H et al. (2010) Long fire cycle in northern boreal *Pinus* forests in Finnish Lapland. *Canadian Journal of Forest Research* 40: 2027–2035.
- Wanamaker AD Jr, Butler PG, Scourse JD et al. (2012) Surface changes in the North Atlantic meridional overturning circulation during the last millennium. *Nature Communications* 3: 899, doi:10.1038/ncomms1901.
- Witter JB and Self S (2007) The Kuwae (Vanuatu) eruption of AD 1452: Potential magnitude and volatile release. *Bulletin of Volcanology* 69: 301–318.
- Young GHF, McCarroll D, Loader NJ et al. (2010) A 500 year record of near-ground solar radiation from tree-ring stable carbon isotopes. *The Holocene* 20: 315–324.
- Young GHF, McCarroll D, Loader NJ et al. (2012) Changes in atmospheric circulation and the Arctic Oscillation preserved within a millennial length reconstruction of summer cloud cover from northern Fennoscandia. *Climate Dynamics* 39: 495–507.
- Zhong Y, Miller GH, Otto-Bliesner BL et al. (2011) Centennial-scale climate change from decadal-paced explosive volcanism: A coupled sea ice-ocean mechanism. *Climate Dynamics* 37: 2373–2387.